Welding Letters Vol.41 No.4 (2023) p.9 WL-12 WL DOI: 10.2207/qjjws.41.9WL

Experimental comparison on load-carrying capacity of corner joints by laser-arc hybrid welding and arc welding

Gang Chen[a], Mikihito Hirohata[a,*], Kengo Hyoma[b], Naoyuki Matsumoto[b] and Koutarou Inose[b]

[a] *Division of Global Architecture, Graduate School of Engineering, Osaka University, Osaka, Japan*
[b] *IHI Corporation, Yokohama, Japan*

For extending the application of hybrid welding to the fabrication of steel bridge structures, a series of experiments were performed. One-pass full-penetration corner joints of SBHS500 with 12 mm thickness were fabricated by laser-arc hybrid welding. Four passes were required to produce the same-dimensional full-penetration corner joints by conventional arc welding. Monotonic compressive loading experiments were performed to investigate the load-carrying performances of hybrid-welded and arc-welded corner joints. Compared to arc-welded specimens, the elastic stiffness of hybrid-welded specimens was greater by 24%, and the maximum compressive load of hybrid-welded specimens was greater by 5%, demonstrating that the load-carrying performances of hybrid-welded corner joints may outperform arc-welded corner joints.

Key Words: Laser-arc Hybrid Welding, Bridge, Corner Joints, Deformation, Residual Stress

1. INTRODUCTION

Laser-arc hybrid welding, which is an effective combination of laser and arc welding, offers many advantages over laser- or arc-only welding. Hybrid welding increases gap tolerance when compared with laser welding[1]. Moreover, compared to arc welding, hybrid welding features high travel speed, deep penetration, and low heat input[2-4]. Therefore, hybrid welding is predicted to be widely used to fabricate steel bridge structures.

Steels for Bridge High-performance Structures (SBHS), which feature higher yield stress, greater toughness, and weldability than conventional steel grades, were specified by JIS G3140 in 2008. SBHS is expected to be widely applied to construct steel bridge structures to decrease construction costs and improve the service life of steel bridges.

The authors have noted the combination of hybrid welding and SBHS by anticipating a synergy between high-quality welding processes and high-performance materials. In previous studies[5, 6], a series of experiments were conducted to examine the basic characteristics of the hybrid-welded joints of SBHS and to measure the welding deformation and residual stress of the joints. Numerical simulations were performed to obtain a detailed distribution of the residual stress of the hybrid welded joints. However, few experimental studies on load-carrying performances have directly compared hybrid-welded joints with arc-welded joints. This study compares the load-carrying performance of hybrid-welded corner joints with that of arc-welded corner joints of an SBHS through monotonic compression loading experiments.

received ver: 2023.05.11 ; accepted: 2023.6.26
*Corresponding author
E-mail address: hirohata@civil.eng.osaka-u.ac.jp

2. FABRICATION OF SPECIMENS

Figure 1 illustrates the geometry of corner joints. The steel plates were SBHS500 with 12 mm thickness. The hybrid-welded specimens had a gap of 0.5 mm between the plates to be welded. Previous study indicated that hybrid welding allows for the bridging of maximum gap widths of 0.8 mm in structural steels with a thickness of 15 mm[7]. The gap width of 0.5mm selected in this study followed to this previous study. The arc-welded specimens had a single 45° bevel and a root face of 1mm. The plates at the top and

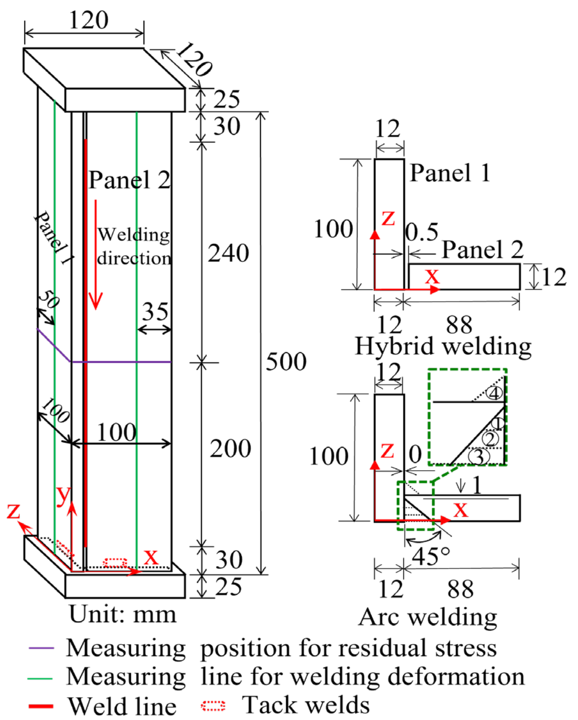

Fig. 1 Experimental specimen

Table 1 Chemical compositions and mechanical properties of SBHS500 and filler material

	Grade	Chemical compositions [mass %]								Yield strength [N/mm^2]	Tensile strength [N/mm^2]	Elongation [%]
		C	Si	Mn	P	S	Ni	Cr	Cu			
Base metal	SBHS500	0.10	0.22	1.54	0.014	0.002	0.02	0.14	0.01	587	684	35
Filler material	YGW11	0.08	0.51	1.10	0.010	0.010	—	—	—	490	570	31

Table 2 Welding conditions

Welding process	Welding pass	Laser power [kW]	Arc current [A]	Arc voltage [V]	Welding speed [m/min]	Heat input [J/mm]		
						Laser	Arc	Total
Hybrid	1	6.8	230	23.8	1.2	340	274	614
Arc	1	—	175	24.5	0.35	—	735	7652
	2	—	250	30.5	0.35	—	1307	
	3	—	250	31.0	0.20	—	2325	
	4	—	300	36.5	0.20	—	3285	

bottom of the specimens were connected to Panels 1 and 2 by tack welding at the positions shown in Figure 1. The plates at the top and bottom were just for load transfer in subsequent loading experiments. For minimizing the influence of connecting these plates to Panels 1 and 2 on the residual stress distributions, the plates were connected by tack welding only.

Table 1 lists the chemical composition and mechanical properties of the base metal and filler material. The corner joints were assembled using two steel plates through hybrid and arc welding, forming an L-shaped cross-section.

Figure 2 shows the hybrid welding process. The shielding gas used for hybrid welding and arc welding was 100% CO_2. The arc torch preceded the laser. One-pass full penetration was achieved by hybrid welding under the welding conditions listed in Table 2. For the arc welding, three passes were performed on the machined groove sides of the corner joints. Subsequently, gouging and a final welding pass were performed from the rear. Four passes were required to produce the same-dimensional full penetration using arc welding. Four hybrid-welded corner joints and four arc-welded corner joints were used. The posture of the hybrid welding was horizontal. The posture of all passes of the arc welding was downward.

Figure 3 shows cross-sectional macroscopic photographs of the hybrid-welded and arc-welded corner joints. Upon visual inspection, no welding defects were observed in either type of welded joint. Hybrid welding features deeper penetration than arc-only welding, making single-pass full penetration of thick steel plates possible. This is in stark contrast to arc welding, which requires four passes to achieve full penetration.

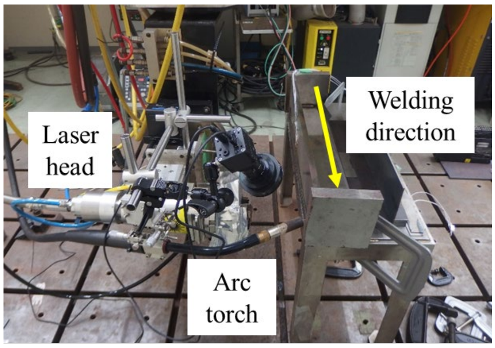

Fig. 2 Appearance of hybrid welding process

3. EXPERIMENTAL PROCEDURE AND RESULTS

3.1 Welding deformation

A digital depth gauge was applied from a reference rigid frame to measure welding deformation. The out-of-plane deformations of the panels were measured along the y-direction before and after welding on the lines of x = 0 mm and z = 50 mm for Panel 1 and the line of x = 65 mm and z = 0 mm for Panel 2. The difference between them corresponds to welding deformation. Figure 4 shows the out-of-plane welding deformations. The deformations are the average values of the four hybrid- and four arc-welded specimens. For Panel 1, the maximum values of the welding out-of-plane deformation of hybrid-welded and arc-welded joints were 0.67 mm and 2.37 mm, respectively. As for Panel 2, the maximum values of the welding out-of-plane deformation of hybrid-welded and arc-welded specimens were 0.47 mm and 1.87 mm. The welding deformation of the hybrid-welded specimens was approximately 70% less than that of the arc-welded specimens because the heat input of hybrid welding was less than that of arc welding, as shown in Table 2.

3.2 Residual stress

The residual stress was measured using X-ray diffraction on the x = 0, y = 230, z = 2.5, 7.5, 12.5, 17.5, 22.5, 27.5, 32.5, 37.5, 47.5, 57.5, 67.5, 77.5, 87.5 in Panel 1 for hybrid- and arc-welded specimens, on the x = 2.5, 20, 25, 30, 35, 40, 45, 50, 55, 60, 65, 75, 85, 95mm, y = 230 mm, z = 0 mm for hybrid-welded specimens, and on the x=2.5, 30, 35, 40, 45, 50, 55, 60, 65, 75, 85, 95 mm, y = 230 mm, z = 0 mm for arc-welded specimens. Before measuring residual stress, to eliminate the influence of surface processing, the area around measuring positions was electropolished to roughly 300 μm depth. Figure 5 shows the stress components of Panels 1 and 2 in the welding direction. The light blue area represents the weld bead region in arc welding, while the light red area represents the weld bead region in hybrid welding. The residual stresses are the average values of the four hybrid- and four arc-welded specimens. As shown in the figure, the residual stresses on the weld bead were not measured. The stresses were measured at the two surfaces of Panels 1 and 2. Even though the influence of the bending deformation could not be eliminated, for Panel 1, the maximum compressive residual stress in hybrid-welded and arc-welded joints were -143.3 N/mm^2 and -307.8 N/mm^2, respectively. As for Panel 2, the maximum compressive residual stress in hybrid-welded and arc-welded specimens was -105.5 N/mm^2 and -188 N/mm^2, respectively. The maximum compressive residual stress of the hybrid-welded specimens was approximately 50% lower than that of the arc-welded specimens. For the hybrid-welded specimens, tensile residual stress was generated near the welds owing to contraction during the rapid cooling process, a phenomenon that can be clearly observed in Panel 2. For the arc-welded specimens, a small residual stress was observed in the vicinity of the welds because the thermal cycles, which were imposed by neighboring welding passes, served as a local heat treatment that could effectively relieve the residual stress. Furthermore, the welding out-of-plane deformation might apply the bending stresses to Panels 1 and 2. The tendency of the welding deformation was convex to the positive directions in the x and z axes. The compressive stress might be superimposed to the surfaces of Panels 1 and 2 at which the residual stresses were measured. It might be another reason for the small residual stress around the weld bead.

3.3 Load-carrying capacity

To elucidate the load-carrying capacity of the hybrid-welded corner joints, monotonic compression loads were applied to the specimens in the vertical direction, as shown in Figure 6. A displacement meter was installed between the top and bottom centers of the loading plates to monitor the vertical displacement. The three hybrid-welded specimens exhibited similar tendencies in the relationship between load and vertical displacement, as did the three arc-welded specimens. Therefore, a representative experimental result (specimen No. 1) is shown in Figure 7. In this study, the elastic stiffness was determined using linear regression within a load range of 400kN to 800kN, which was selected as the calculation interval. The average values of the elastic stiffness of three hybrid-welded and three arc-welded specimens were 864.8 kN/mm and 698.1 kN/mm, respectively. The elastic stiffness of the hybrid-welded specimens was approximately 24% higher than that of the arc-welded specimens. This may be due to the difference in the magnitude of welding deformation. The welding deformation corresponds to the initial geometric imperfection in the loading process, which largely influences the elastic stiffness and the maximum load. As listed in Table 2, arc-welded corner joints experienced larger heat input than hybrid-welded specimens during the welding process, leading to substantial welding deformation. This increased welding deformation introduced additional strains and displacements, resulting in a reduction of structural stiffness. In contrast, hybrid-welded corner joints exhibited less welding deformation and, consequently, has a lesser influence on the elastic stiffness. The average values of the maximum compressive loads of three hybrid-welded and three arc-welded corner specimens were 1343 kN and 1280 kN, respectively. The maximum compressive loads of the hybrid-welded specimens were approximately 5% higher than those of the arc-welded specimens. In addition to the

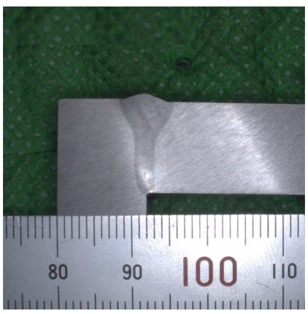

(a) Hybrid welding

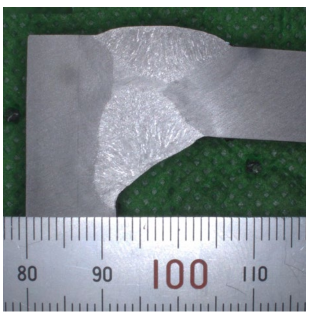

(b) Arc welding

Fig. 3 Macroscopic photographs

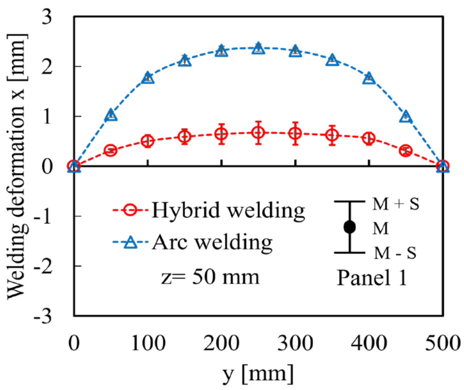

(a) Panel 1

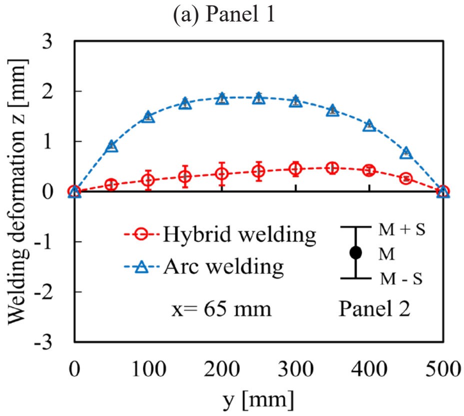

(b) Panel 2

Fig. 4 Welding deformation

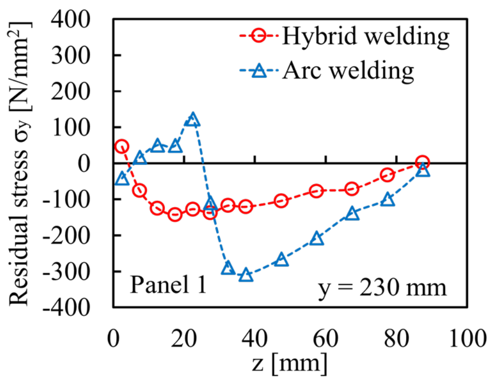

(a) Panel 1

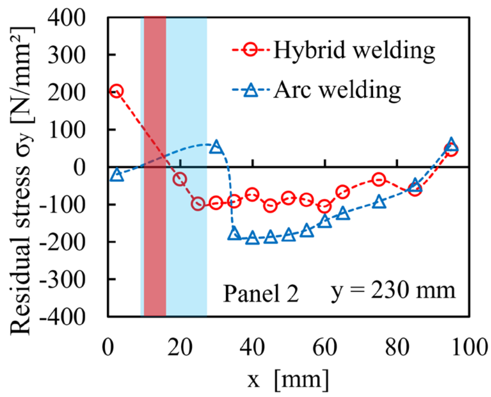

(b) Panel 2

Fig. 5 Residual stress

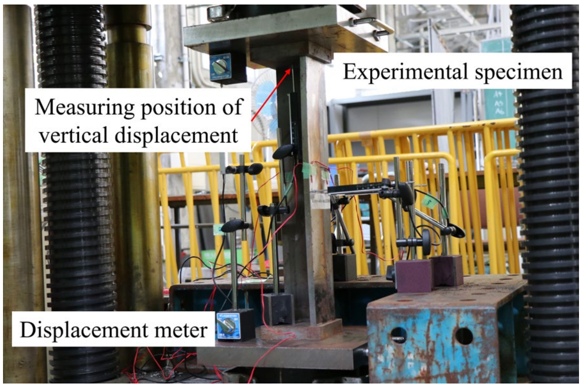

Fig. 6 Setup of compressive loading experiment

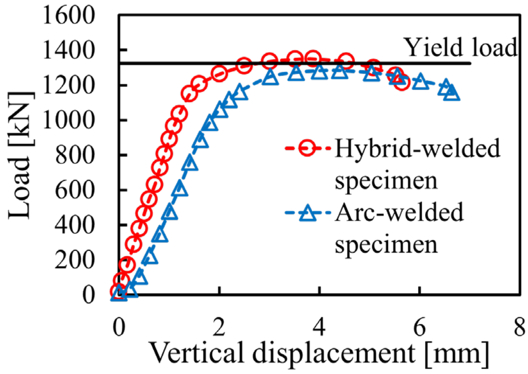

Fig. 7 Relationship between load and vertical displacement

difference in the magnitude of welding deformations between the hybrid- and arc-welded specimens, this may be due to the difference in the compressive residual stresses between them. The compressive residual stress σy was an influential factor that could affect the maximum compressive loads. As shown in Fig. 5, the compressive residual stress σy in the arc-welded specimens was higher than that in the hybrid-welded specimens. This leads to the earlier yielding of the arc-welded specimens compared to the hybrid-welded specimens in the loading experiment, thereby limiting the maximum compressive loads that the arc-welded specimens can sustain. Therefore, the load-carrying performance of the hybrid-welded corner joints may outperform that of the arc-welded corner joints in combination with no visible welding defects in the cross-sectional macroscopic photographs of the hybrid-welded and arc-welded corner joints.

In this study, the primary investigation focused on the deformation, residual stress, and load-carrying capacity of hybrid-welded corner joints. Further investigations will be undertaken in the future through numerical simulations to elucidate the tendencies of the deformation and residual stress. Based on these results, changes in the load-carrying capacity will be examined.

4. CONCLUSIONS

A series of measurements and monotonic compressive loading experiments were performed to investigate the load-carrying capacity of hybrid-welded corner joints using an SBHS. The main results are as follows:

(1) A one-pass full-penetration corner joint of SBHS500 with a thickness of 12 mm was fabricated using hybrid welding. Four passes were required to produce same-dimensional full-penetration corner joints via arc welding.

(2) The welding deformation of the hybrid-welded joints was approximately 70% less than that of the arc-welded joints. The maximum compressive residual stress of the hybrid-welded joints is approximately 50% lower than that of the arc-welded joints.

(3) The load-carrying performances of the hybrid- and arc-welded corner joints were examined via monotonic compressive loading experiments. Compared with the arc-welded joints, the average elastic stiffness of the hybrid-welded specimens increased by 25%, and the maximum mean compressive load of the hybrid-welded specimens increased by 5%.

Acknowledgements

This research was part of the activities carried out by an ad hoc research group at the Japan Welding Society. This research was supported by JST SPRING, Grant Number JPMJSP2138.

References

1) Üstündağ Ö, Fritzsche A, Avilov V, Gumenyuk A and Rethmeier M: Study of gap and misalignment tolerances at hybrid laser arc welding of thick-walled steel with electromagnetic weld pool support system, Procedia Cirp, 74 (2018),757–760.

2) Uemura T, Gotoh K and Uchino I: Expansion of laser-arc hybrid welding to horizontal and vertical-up welding, Weld World, 66 (2022), 495–506.

3) Bunaziv I, Akselsen O, Frostevarg J and Kaplan A: Application of laser-arc hybrid welding of steel for low-temperature service, The International Journal of Advanced Manufacturing Technologies, 102 (2019), 2601–2613.

4) Üstündağ Ö, Bakir N, Gook S, Gumenyuk A and Rethmeier M: Hybrid laser-arc welding of laser- and plasma-cut 20-mm-thick structural steels, Weld World, 66 (2022), 507–514.

5) Hirohata M, Chen G, Morioka K, Hyoma K, Matsumoto N and Inose K: An Investigation on laser-arc hybrid welding of one-pass full-penetration butt-joints for steel bridge members, Welding in the World, 66 (2021), 515-527.

6) Chen G, Sakai N, Hirohata M, Hyoma K, Matsumoto N and Inose K: Bending Fatigue Characteristics of Butt Joints by Laser-Arc Hybrid Welding for Steel Bridge Members, Vehicle and Automotive Engineering 4 (2022), 904-916.

7) Kristensen J K: Thick Plate CO2-Laser based Hybrid Welding of Steels, Weld World, 53 (2009), 47-57.